MICROSTRUCTURE AND PROPERTIES OF $Y_{0.1}Sr_{0.9}CoO_{3-x}$ THIN FILMS PRODUCED BY HIGH-FREQUENCY LASER DEPOSITION

N. A. Bosak,[a,*] A. N. Chumakov,[a] M. V. Bushinsky,[b] G. M. Chobot,[c] L. V. Baran,[d] A. A. Shevchenok,[c,f] V. V. Malyutina-Bronskaya,[e] and A. A. Ivanov[a]

UDC 621.373.826;533.216.2

Nanostructured thin films on a silicon substrate were obtained by high-frequency pulse-periodic (f ~ 8–10 kHz) action of a laser with wavelength λ = 1.064 μm and power density q = 36 MW/cm^2 on $Y_{0.1}Sr_{0.9}CoO_{3-x}$ ceramics in a vacuum chamber at pressure p = 2·10^{-2} mm Hg. Their morphology was studied using atomic force microscopy. Features of their transmission spectra in the visible and near- and mid-IR regions were revealed. The electrophysical properties of the $Y_{0.1}Sr_{0.9}CoO_{3-x}$ structures were analyzed.

Keywords: *high-frequency laser irradiation, thin-film structure, transmission and reflection spectra, electrophysical characteristics.*

Introduction. Complex metal-oxide compounds with reproducible physicochemical properties under various external effects are currently widely researched. Among the variety of such compounds, complex cobalt oxides $Ln_{1-x}A_xCoO_{3-\delta}$ (Ln = lanthanide, A = alkaline-earth ion) with the perovskite structure are attracting heightened interest because of the coupling between their magnetic and transport properties [1], colossal magnetoresistance [2], metal–dielectric and antiferromagnetic– ferromagnetic transitions [3], spin crossover, unusual types of magnetic ordering, etc. [4–6]. Such materials are promising for solid-state power sources, oxygen membranes, thermoelectric elements, cathode materials, and gas and field sensors and for application in spintronic devices etc. [7]. Furthermore, metal oxides are used in optoelectronics [8, 9].

Compositions $R_xSr_{x-1}CoO_3$ (R = rare-earth ion) are interesting because their crystal structure and magnetic and electric properties depend on the degree of substitution, oxygen stoichiometry, and temperature. Compositions $Y_xSr_{x-1}CoO_3$ are studied most because they exhibit ferromagnetic properties up to ambient temperatures [10–13]. The crystal and magnetic structure and magnetic and magneto-transport properties of these compositions are well studied [9–14]. However, their optical properties have not been examined in detail [15].

The present work investigated thin films of $Y_{0.1}Sr_{0.9}CoO_{3-x}$ deposited under vacuum onto a silicon substrate using multi-pulse high-frequency laser action [16]. The morphology of the obtained thin films was studied using atomic force microscopy (AFM). Features of transmission spectra in the near- and mid-IR regions and reflection spectra in the visible and near-IR regions were found. The voltammetric characteristics (VAC) and volt–Faraday characteristics (VFC) were investigated. Data from additional studies of transmission spectra in the near- and mid-IR regions and reflection spectra in the visible and near-IR regions of the silicon substrate revealed features of spectra of the silicon substrate with a deposited nanostructured film of $Y_{0.1}Sr_{0.9}CoO_{3-x}$.

Experimental. A polycrystalline $Sr_{0.9}Y_{0.1}CoO_{3-\gamma}$ target was synthesized by solid-state ceramic technology in air. The starting oxides Y_2O_3 and Co_3O_4 and $SrCO_3$ (high-purity, analytically pure) were taken in the stoichiometric ratio

[*]To whom correspondence should be addressed.

[a]B. I. Stepanov Institute of Physics, National Academy of Sciences of Belarus, Minsk, Belarus; email: n.bosak@ifanbel.bas-net.by; [b]NPC of the National Academy of Sciences of Belarus for Materials Science, Minsk, Belarus; email: bushinsky@physics.by; [c]Belarusian State Agrarian Technical University, Minsk, Belarus; [d]Belarusian State University, Minsk, Belarus; email: baran@bsu.by; [e]SSPA Optics, Optoelectronics, and Laser Technology, Minsk, Belarus; email: malyutina@oelt.basnet.by; [f]Belarusian National Technical University, Minsk, Belarus; email: alexshev56@mail.ru. Translated from Zhurnal Prikladnoi Spektroskopii, Vol. 90, No. 1, pp. 43–47, January–February, 2023. Original article submitted October 24, 2022; https://doi.org/10.47612/0514-7506-2023-90-1-43-47.

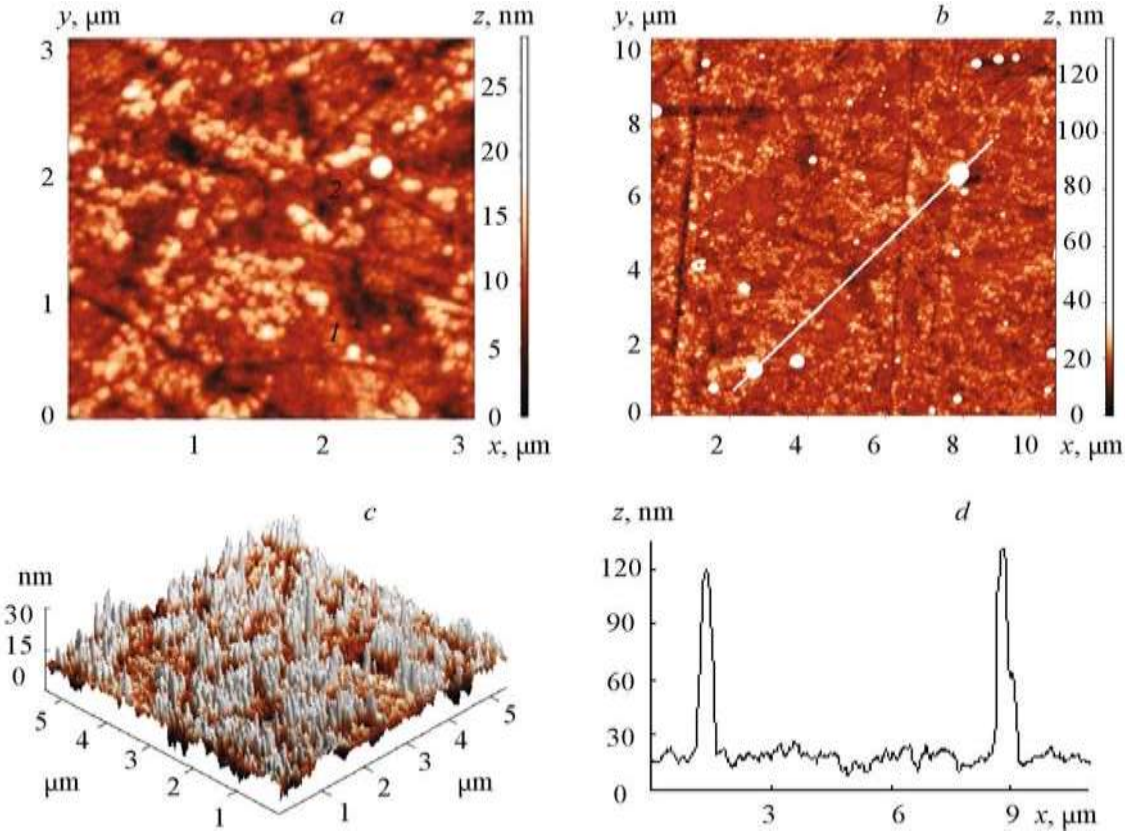

Fig. 1. AFM images of the surface of laser-deposited thin film of $Y_{0.1}Sr_{0.9}CoO_{3-x}$ (a–c) and cross-section profile of relief along the indicated line (d).

and thoroughly mixed in a RETSCH PM-100 planetary ball mill for 30 min at 250 rpm. Y_2O_3 was preliminarily annealed at 1000°C to remove moisture before weighing. Samples were synthesized in two steps. A preliminary synthesis used a temperature of 1000°C. The sample was ground and pressed into a pellet of diameter ~ 20 mm. The final synthesis of the target used a temperature of 1185°C for 8 h. Then, the target was cooled for 12 h to 300°C. X-ray structure studies of the obtained target were made at room temperature on a DRON-3M diffractometer in CuK_α-radiation and showed no extraneous phases.

Films of $Y_{0.1}Sr_{0.9}CoO_{3-x}$ were deposited by high-frequency laser sputtering of the ceramic target under vacuum ($p = 2 \cdot 10^{-2}$ mm Hg). The experimental laser system ($\lambda = 1.06$ μm) with the pulse rate regulated from 5 to 50 kHz contained a laser-radiation source, an optical system for transporting the laser radiation to the target being sputtered, a vacuum chamber, and a measurement and diagnostic module. The pulse rate was varied by varying the laser pumping level and optical density of a gate of irradiated crystalline lithium fluoride (LiF) with F_2^- color centers. The pulse length at half-height was $\tau \sim 85$ ns. Macroscopically uniform thin films were deposited at laser-radiation power density $q = 36$ MW/cm^2 and pulse rate $f \sim 8$–10 kHz.

The surface morphology of the samples was studied using a Solver P47-Pro scanning probe microscope (NT-MDT, Russia) in amplitude-modulated mode. Transmission of optical radiation by the thin films in the near-IR regionwas measured on a Cary 500 Scan spectrophotometer. Transmission spectra in the mid-IR region were recorded using a NEXUS FT-IR spectrometer (Thermo Nicolet) in the range 400–4000 cm^{-1}. VAC and VFC were measured using an E7-20 automated immittance meter at room temperature. VFC were measured at signal frequencies 100 and 500 kHz and 1 MHz.

Results and Discussion. AFM established the nanocrystalline structure of $Y_{0.1}Sr_{0.9}CoO_{3-x}$ thin films obtained by high-frequency laser sputtering of the ceramic target (Fig. 1). The average drop of heights determined at five different points on the sample (scan region 10 × 10 μm) was 57 nm with an average squared roughness of 14.5 nm. An insignificant number of large particles of height up to 130 nm and lateral size 100–200 nm was observed on the film surface. The average lateral size of the film structural elements was 40 nm.

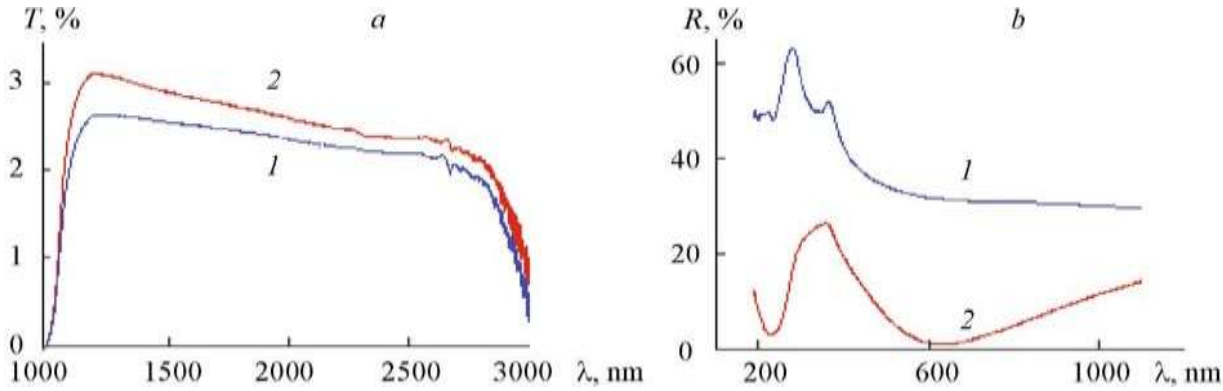

Fig. 2. Transmission (a) and reflection spectra (b) of silicon (1) and laser-deposited film of $Y_{0.1}Sr_{0.9}CoO_{3-x}$ on silicon substrate (2) in visible and near-IR regions.

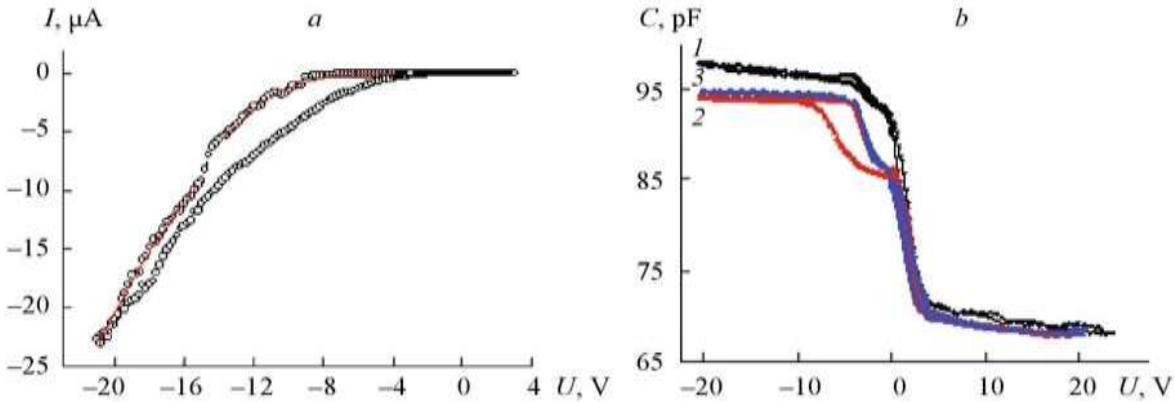

Fig. 3. Voltammetric (a) and volt-faradaic characteristics (b) of thin film of $Y_{0.1}Sr_{0.9}CoO_{3-x}$ in silicon substrate at signal frequencies 100 (1), 500 (2), and 1000 kHz (3).

The transmission of the laser-deposited film of $Y_{0.1}Sr_{0.9}CoO_{3-x}$ on silicon in the near-IR region fell from T = 3.1% at λ = 1198 nm to T = 2.3% at λ = 2400 nm (Fig. 2a). The reflection coefficient of the $Y_{0.1}Sr_{0.9}CoO_{3-x}$ film reached a maximum of R_{max} = 26.5% at λ = 361 nm with a subsequent decrease to R_{min} = 1.03% at λ = 631 nm and an increase to R_{max} = 14.3% at λ = 1100 nm (Fig. 2b). The reflection spectrum exhibited two broad absorption bands near 227 and 631 nm.

The presence of localized electronic states in the nanostructured film could affect the establishment of a current through the structure. Figure 3a shows the VAC of a $Y_{0.1}Sr_{0.9}CoO_{3-x}$ thin film on silicon. Hysteresis and two portions that were described by a power dependence of current on potential (characteristic for a current limited by space charge in an oxide film with deep traps) could be identified with a negative potential applied to the film, i.e., $I \sim U^m$, where m = 3 for potential U from –4 to 7.8 V, m = 4.6 for U from –8 to –14.8 V, and m = 2.7 for U from –15 to –21 V [17]. The VFC were measured at various frequencies to confirm the presence of deep electronic states in the layer of the $Y_{0.1}Sr_{0.9}CoO_{3-x}$ thin film and at the interface. Figure 3b shows the VFC of the $Y_{0.1}Sr_{0.9}CoO_{3-x}$/Si structure. Hysteresis that was ~ 1 V at a signal frequency of 100 kHz, ~3 V, at 500 kHz, and 0, at 1 MHz, was observed in the VFC in the capacity modulation region at negative potentials. This may have been related to surface states contributing to the overall capacitance at just this frequency because the capacitance of the MOS structure did not change after 500 kHz. Therefore, 500 kHz was a rather high frequency of variable potential where minor charge carriers could not accumulate after the potential change. A feature as a step of the VFC in the capacitance modulation region from –3 to 0 V may also have been related to the nanocrystalline structure of the film caused by deep traps in the dielectric that also created hysteresis in the VFC and VAC [18].

Conclusions. Nanocrystalline $Y_{0.1}Sr_{0.9}CoO_{3-x}$ films with structural elements of average lateral size 40 nm and average squared roughness of 14.5 nm were prepared by high-frequency laser sputtering. The transmission of a laser-deposited $Y_{0.1}Sr_{0.9}CoO_{3-x}$ film on silicon in the near-IR region fell from T = 3.1% at λ = 1198 nm to T = 2.3% at λ = 2400 nm. The reflection coefficient of the $Y_{0.1}Sr_{0.9}CoO_{3-x}$ film reached a maximum R_{max} = 26.5% at λ = 361 nm and a minimum R_{min} = 1.03% at λ = 631 nm. Two broad absorption bands near 227 and 631 nm were observed in the reflection spectrum. The electrical properties of the studied film on silicon showed mono-energetic surface states in the bandgap. These surface states were due to the crystal structure of the oxide film at the $Y_{0.1}Sr_{0.9}CoO_{3-x}$/Si interface.

REFERENCES

1. N. B. Ivanova, S. G. Ovchinnikov, M. M. Korshunov, I. M. Eremin, and N. V. Kazak, *Usp. Fiz. Nauk*, **179**, 837–860 (2009).
2. A. Maignan, C. Martin, D. Pelloquin, N. Nguyen, and B. Raveau, *J. Solid State Chem.*, **142**, No. 2, 247–260 (1999).
3. I. O. Troyanchuk, N. V. Kasper, D. D. Khalyavin, H. Szymczak, and M. Baran, *Phys. Rev. Lett.*, **80**, 3380–3383 (1998).
4. I. O. Troyanchuk, D. V. Karpinsky, A. P. Sazonov, V. Sikolenko, V. Efimov, and A. Senyshyn, *J. Mater. Sci.*, **44**, 5900–5908 (2009).
5. I. O. Troyanchuk, M. V. Bushinsky, N. V. Tereshko, R. A. Lanovsky, V. V. Sikolenko, C. Ritter, Yu. S. Orlov, and S. G. Ovchinnikov, *Mater. Res. Express*, **6**, Article ID 026105 (2019).
6. D. D. Khalyavin, D. N. Argyriou, U. Amann, A. A. Yaremchenko, and V. V. Kharton, *Phys. Rev. B: Condens. Matter Mater. Phys.*, **75**, Article ID 134407 (2007).
7. C. A. Hancock, R. C. T. Slade, J. R. Varcoe, and P. R. Slater, *J. Solid State Chem.*, **184**, 2972–2977 (2011).
8. G. Blasse, *Mater. Chem. Phys.*, **16**, Nos. 3–4, 201–236 (1987).
9. C. Greskovich and S. Duclos, *Annu. Rev. Mater. Sci.*, **27**, 69–88 (1997).
10. S. Fukushima, T. Sato, D. Akahoshi, and H. Kuwahara, *Appl. Phys.*, **103**, Article ID 07F705s07F709 (2008).
11. I. O. Troyanchuk, M. V. Bushinskii, V. M. Dobryanskii, and N. V. Pushkarev, *Pis'ma Zh. Eksp. Teor. Fiz.*, **94**, No. 12, 930–933 (2011).
12. I. O. Troyanchuk, M. V. Bushinskii, R. A. Lanovskii, V. V. Sikolenko, and K. Ritter, *Fiz. Tverd. Tela*, **60**, No. 10, 1957–1963 (2018).
13. R. Lanovsky, N. Tereshko, O. Mantytskaya, V. Fedotova, D. Kozlenko, C. Ritter, and M. Bushinsky, *Phys. Status Solidi B*, Article ID 2100636 (2022).
14. V. Sikolenko, I. Troyanchuk, M. Bushinsky, V. Efimov, L. Keller, J. S. White, F. R. Schilling, and S. Schorr, *J. Phys.: Cond. Matter*, **27**, Article ID 046005 (2015).
15. A. A. Moez and A. I. Ali, *J. Mater. Sci.: Mater. Electron.*, **32**, Article ID 19275 (2021).
16. L. Ya. Min′ko, A. N. Chumakov, and N. A. Bosak, *Kvantovaya Élektron. (Moscow)*, **17**, No. 11, 1480–1484 (1990).
17. N. A. Bosak, A. N. Chumakov, A. A. Shevchenok, L. V. Baran, V. V. Malyutina-Bronskaya, A. G. Karoza, and A. A. Ivanov, *Zh. Bel. Gos. Univ., Fiz.*, **2**, 10–18 (2020).
18. N. A. Bosak, A. N. Chumakov, M. V. Bushinskii, G. M. Chobot, L. V. Baran, A. A. Shevchenok, V. V. Malyutina-Bronskaya, and A. A. Ivanov, in: *Proc. Int. Symp. "Promising Materials and Technologies,"* August 23–27, 2021, Minsk, Belarus (2021), pp. 187–189.